



# Rapid titanium carbide synthesis from titanium and graphite powders via ultrafast high-temperature sintering

Daiki Akutagawa<sup>a</sup>, Toshiki Sato<sup>a</sup>, Tomoharu Tokunaga<sup>a</sup>, Kiyoshi Kobayashi<sup>b</sup>,  
Takahisa Yamamoto<sup>a,\*</sup>

<sup>a</sup> Department of Materials Design Innovation Engineering, Nagoya University, Furo-cho, Chikusa-ku, Nagoya 464-8603, Japan

<sup>b</sup> Research Center for Electronic and Optical Materials, National Institute for Materials Science, Sengen 1-2-1, Tsukuba, Ibaraki 305-0047, Japan

## ARTICLE INFO

### Keywords:

Titanium carbide  
Graphite  
Ultrafast high-temperature sintering  
Self-propagating high-temperature synthesis

## ABSTRACT

Self-propagating high-temperature synthesis (SHS) is a combustion-based method that involves a self-heating chain reaction, which is effective for rapidly producing materials with high melting points. Herein, ultrafast high-temperature sintering (UHS) was leveraged to ignite the SHS of titanium carbide (TiC) from titanium and graphite powders, and the heat generation and microstructural evolution during the process were investigated. The exothermic heat generated during TiC synthesis was confirmed, demonstrating that SHS was initiated in the initial stage of UHS. The incubation time before SHS ignition decreased with an increase in the UHS temperature above the melting point of titanium. Scanning electron microscopy revealed that fine TiC grains formed during SHS, which became denser under continued UHS. Additionally, molten Ti spread over the graphite particles during SHS, which transformed into plate-like TiC grains with elongated voids between them under subsequent heating by UHS. This structural feature was found to hinder further densification.

## 1. Introduction

Self-propagating high-temperature synthesis (SHS) relies on combustion and is self-driven by the heat generated during exothermic reactions between the raw elements, making it an attractive method from the perspective of energy conservation [1–3]. TiC, which has a high modulus, hardness, and melting point [4], has been intensively studied as a model material for SHS because 184 kJ/mol of heat is released during the reaction of  $\text{Ti} + \text{C} \rightarrow \text{TiC}$  [5,6]. To ignite a self-propagating chain reaction for SHS, it is necessary to induce the first reaction via resistance heating, laser irradiation, arcing, or any other method of ignition [7–9]. In this study, we applied ultrafast high-temperature sintering (UHS) to initiate SHS in a green compact comprising titanium and graphite powders. The UHS, which uses carbon felt as a heater material, is capable of significant rapid heating up to 2000 °C within approximately 1 s and can easily achieve a very low oxygen partial pressure, suitable for producing TiC [10,11]. The heat generation and microstructural formation obtained during UHS-ignited SHS were investigated herein.

## 2. Materials and Methods

Titanium (>99.9 %, 63–90 μm) and graphite powders (>99.9 %, 50 μm) supplied from Kojundo Chemical Laboratory Co., Ltd. were ground and mixed using an agate mortar and pestle, with a Ti:C ratio of 1:1. Disk-shaped green compacts (φ 10 mm × 1 mm) were then sintered in a vacuum (~4 Pa) using a custom UHS apparatus (Fig. 1(a)) [12]. The green compacts were inserted between the upper/lower carbon felt layers (GF-20-2FSH, Nippon Carbon Corporation), which were clamped between two electrodes. The current passing through the carbon felt, supplied using a power supply (PWR1201ML, Kikusui Electronics Industries, Ltd.), and the resulting temperature of the upper carbon felt, measured using a radiation thermometer (FTKX-TNE0240, Japan Sensor Corp.), were simultaneously recorded during UHS. Sample temperatures were estimated based on the upper carbon felt temperature using the finite element method (Autodesk Inventor Professional 2025), as previously described [12]. The sample temperatures corresponding to the carbon felt currents are presented in Fig. 1(b). For each experiment, the current was raised to the set value within 1 s and held for 60 s. The resulting compacts were analyzed by X-ray diffraction (XRD; D2-PHASER, Bruker Corp.) and scanning electron microscopy (SEM;

\* Corresponding author.

E-mail address: [yamamoto.takahisa@material.nagoya-u.ac.jp](mailto:yamamoto.takahisa@material.nagoya-u.ac.jp) (T. Yamamoto).

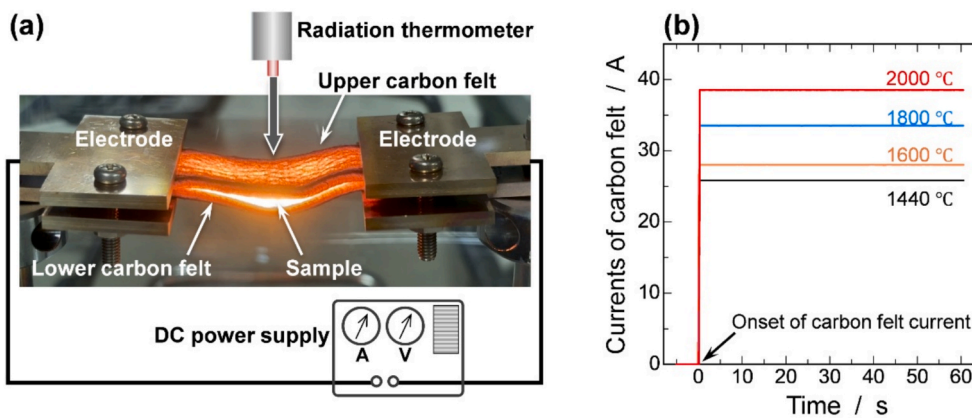


Fig. 1. (a) Illustration of the experimental set-up used for UHS. (b) Diagram of the carbon felt current vs. time, showing the sample temperatures estimated for the respective carbon felt currents.

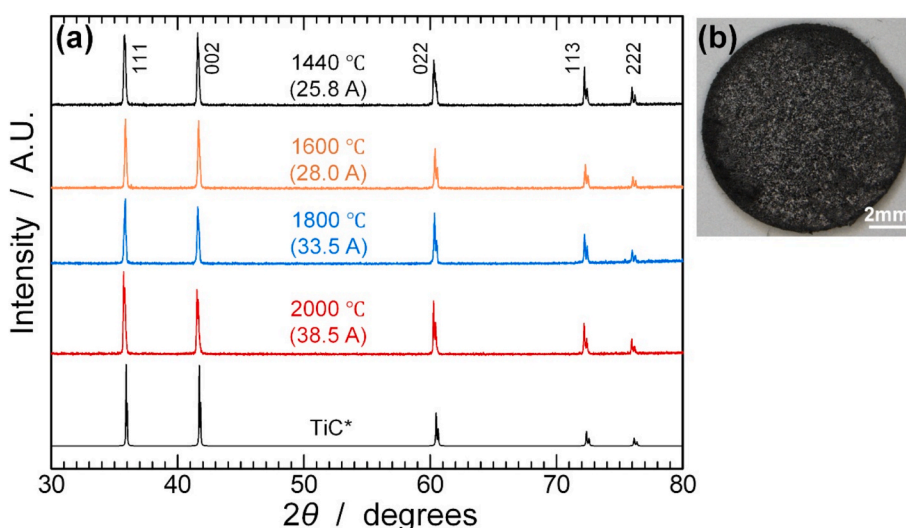


Fig. 2. (a) XRD profiles of the UHS compacts and the referenced profile of TiC [14]. (b) Optical photograph of the compact processed at 2000 °C for 60 s. The values in parentheses indicate the carbon felt currents.

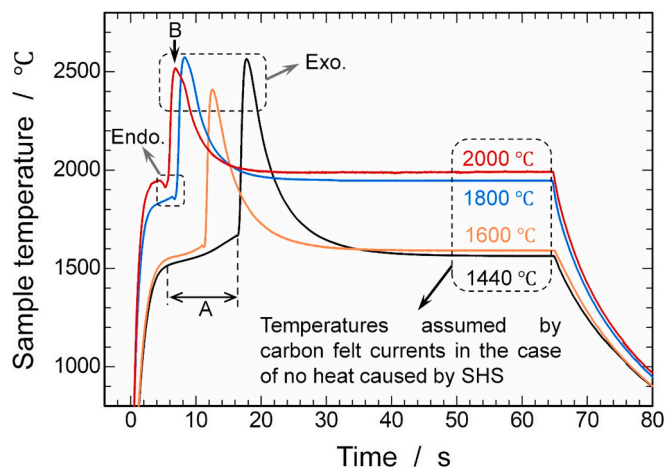


Fig. 3. Sample temperature variation during the UHS process.

MI4000L, Hitachi High-Tech Corp.).

### 3. Results & Discussion

Fig. 2(a) shows XRD profiles of the processed samples, and the diffraction peaks correspond with rock-salt TiC at all sintering temperatures. The lattice constant was  $0.433 \pm 0.0002$  nm, independent of the sintering temperature, consistent with a previous report of stoichiometric TiC (0.432 nm) [13]. In all sample temperature profiles (Fig. 3), a steep temperature rise appears (indicated as Exo.), which is associated with  $Ti + C \rightarrow TiC$ , where the sample temperature becomes higher than that assumed based on the carbon felt current, confirming that UHS can ignite SHS. The samples processed at 1800 and 2000 °C exhibit a slight drop before the Exo. peak (indicated as Endo.). This occurs because the titanium powder melts, considering that the melting point of titanium is 1668 °C [15]. Thus, the initial reaction of  $Ti + C \rightarrow TiC$  involves two cases, depending on the temperature set using the carbon felt current: a reaction between molten titanium and graphite and a reaction between solid titanium and graphite. The period indicated by arrow A corresponds to the incubation time before SHS ignites, which significantly decreases from ~ 10 s at 1440 °C to ~ 1 s at 2000 °C owing to the presence of molten titanium.

Fig. 4 shows cross-sectional SEM images of two sintered compacts: a sintered compact in which the carbon felt current was stopped at the

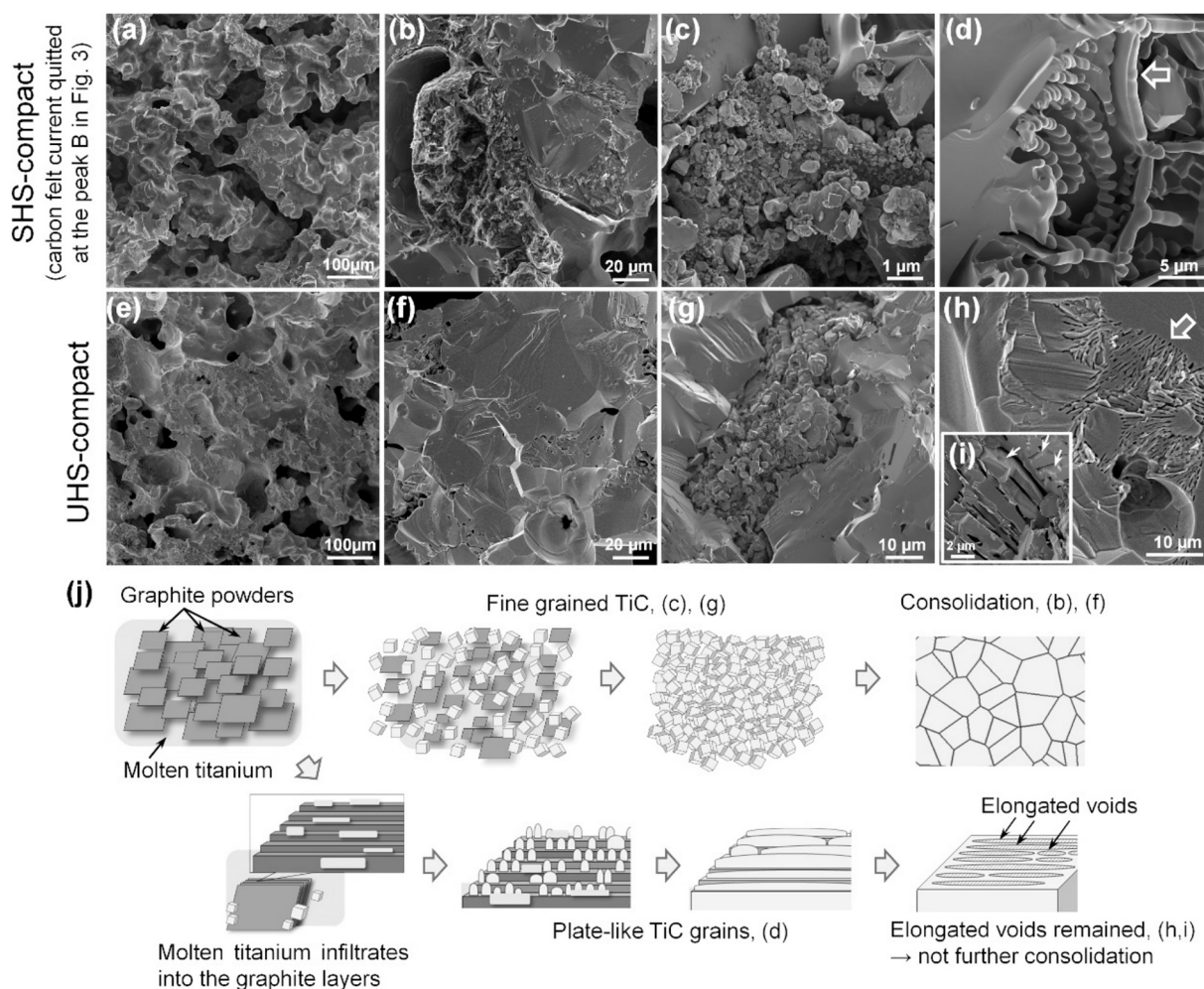


Fig. 4. SEM images of the fractured surface in the (a-d) SHS and (e-i) UHS compacts. (j) Illustration of the change in TiC morphology.

peak of the exothermic reaction (arrow B in Fig. 3), noted as SHS compact in Fig. 4(a-d), and a sintered compact in which the carbon felt current was held for 60 s (along the red line in Fig. 3), noted as UHS compact in Fig. 4(e-i). From the wide-field SEM images (Fig. 4(a, e)), densification progresses under prolonged heating by UHS. Examining the microstructure in the regions where densification has not fully progressed in the SHS compact, two characteristic structures can be identified: a structure in which numerous fine TiC particles are accumulated (Fig. 4(c)) and a structure where molten Ti spreads over the graphite to form smooth surfaces (Fig. 4(d)). Both structures are consistent with previous reports of TiC via SHS [7]. By inspecting the regions of the UHS compact that correspond to each characteristic structure, the structural evolution induced by heat-assisted UHS can be elucidated. The TiC fine particles generated during SHS (Fig. 4(c)) exhibit densification and growth (Fig. 4(g), note the image scale difference between (c) and (g)). The densified regions shown in Fig. 4(b, f) correspond to fully densified TiC particles. In contrast, the structure in Fig. 4(d) has changed to a new characteristic structure consisting of plate-like TiC grains with elongated voids remaining between them (Fig. 4(h, i)). Unlike the regions consisting of fine TiC grains, once the structure shown in Fig. 4(d) is formed in the early stage of SHS, densification barely progresses under continued UHS (Fig. 4(h, i)) because of the elongated voids. According to Lee [7], the structure in Fig. 4(d) corresponds to the spread of molten Ti over graphite. The formation of this structure depends on the morphology of the raw graphite powder. Using graphite in a flake form, a structure like that shown in Fig. 4(d) is more likely to form, which hinders further densification (Fig. 4(h, i), a

side wall of the plate-like TiC grain can be seen in (i)). To promote effective densification under continued UHS, the graphite powder particle size should be minimized to suppress the formation of the characteristic structure shown in Fig. 4(d).

Sun et al. conducted UHS for a green compact comprising TiC powder as the starting material, showing that 2200 °C for 60 s provided a relative density of 78 %, without applying external pressure or observing SHS [16]. In comparison, a lower relative density (roughly 70 % around the body center of the UHS compact) was achieved in the present study using titanium and graphite powders as the starting material. This is attributed to the characteristic structure that forms during SHS (Fig. 4(d, h, i)), which depends on the morphology of the graphite powder used as the raw material. When using titanium and graphite as starting materials in UHS, it is necessary to optimize both the morphology of the graphite powder as well as ensure complete mixing of the titanium and graphite powders [17] and UHS temperature range for the given compact size.

#### 4. Conclusions

A green compact containing titanium and graphite powders was consolidated by UHS, and SHS was confirmed to occur in the early stages, producing TiC. The incubation time before SHS ignition was significantly decreased by increasing the UHS temperature above the melting point of titanium. Microstructural analysis revealed that fine TiC grains were formed during SHS, as well as a structure in which molten titanium spread on graphite. Under continued UHS, the region

composed of fine TiC became denser, but the structure in which molten titanium spread on graphite changed to a structure composed of plate-like TiC with elongated voids, and further densification was not observed. To efficiently densify a green compact made from titanium and graphite powders by UHS-ignited SHS, it is necessary to optimize the morphology of the graphite powder to suppress the formation of the microstructure that inhibits densification.

#### CRedit authorship contribution statement

**Daiki Akutagawa:** Writing – original draft, Investigation, Formal analysis, Data curation. **Toshiki Sato:** Data curation, Conceptualization. **Tomoharu Tokunaga:** Writing – review & editing, Formal analysis, Data curation. **Kiyoshi Kobayashi:** Writing – review & editing, Conceptualization. **Takahisa Yamamoto:** Writing – review & editing, Investigation, Data curation, Conceptualization.

#### Declaration of competing interest

The authors declare that they have no known competing financial interests or personal relationships that could have appeared to influence the work reported in this paper.

#### Acknowledgments

This work was financially supported by CREST (JPMJCR1996) from the Japan Science and Technology Agency.

#### Data availability

The authors do not have permission to share data.

#### References

- [1] A. Makino, Fundamental aspects of the heterogeneous flame in the self-propagating high-temperature synthesis (SHS) process, *Prog. Energy Combust. Sci.* 27 (2001) 1–74, [https://doi.org/10.1016/S0360-1285\(00\)00004-6](https://doi.org/10.1016/S0360-1285(00)00004-6).
- [2] A.S. Mukasyan, et al., Combustion synthesis in nanostructured reactive systems, *Ad. Pow. Tech.* 26 (2015) 954–976, <https://doi.org/10.1016/j.appt.2015.03.013>.
- [3] J. Subrahmanyam, et al., Review self-propagating high-temperature synthesis, *J. Mater. Sci.* 27 (1992) 6249–6273, <https://doi.org/10.1007/BF00576271>.
- [4] A. Saurabh, et al., Titanium-based materials: synthesis, properties, and applications, *Mater. Today: Proc.* 56 (2022) 412–419, <https://doi.org/10.1016/j.matpr.2022.01.268>.
- [5] J.J. Moore, H.J. Feng, Combustion synthesis of advanced materials: part I. reaction parameters, *Prog. Mater. Sci.* 39 (1995) 243–273, [https://doi.org/10.1016/0079-6425\(94\)00011-5](https://doi.org/10.1016/0079-6425(94)00011-5).
- [6] J.J. Moore, H.J. Feng, Combustion synthesis of advanced materials: part II, Classification, Applications and Modeling, *Ibid* 39 (1995) 275–316, [https://doi.org/10.1016/0079-6425\(94\)00012-3](https://doi.org/10.1016/0079-6425(94)00012-3).
- [7] W.C. Lee, S.L. Chung, Ignition phenomena and reaction mechanisms of the self-propagating high-temperature synthesis reaction in the Ti + C system, *J. Mater. Sci.* 30 (1995) 1487–1494, <https://doi.org/10.1007/BF00375253>.
- [8] B. Liang, et al., Synthesis of Ti<sub>2</sub>AlC by laser-induced self-propagating high-temperature sintering, *J. Alloys Compd.* 501 (2010) L1–L3, <https://doi.org/10.1016/j.jallcom.2010.03.218>.
- [9] S. Jin, et al., Self-propagating high-temperature synthesis of nano-TiC particles with different shapes by using carbon nano-tube as C source, *Nanoscale Res. Lett.* 6 (2011) 515. <http://www.nanoscalereslett.com/content/6/1/515>.
- [10] C. Wang, et al., A general method to synthesize and sinter bulk ceramics in seconds, *Science* 368 (2020) 521–526, <https://doi.org/10.1126/science.aaz7681>.
- [11] M. Biesuz, et al., Ultrafast high-temperature sintering (UHS) vs. conventional sintering of 3YSZ: microstructure and properties, *J. Euro. Ceram. Soc.* 44 (2024) 4741–4750, <https://doi.org/10.1016/j.jeurceramsoc.2024.01.064>.
- [12] T. Sato, et al., Healing behavior of microcracks on the surface of yttria-stabilized polycrystals using an ultrafast high-temperature sintering method, *Ceram. Inter.*, 51 (4) 4178–4184. <https://doi.org/10.1016/j.ceramint.2024.11.394>.
- [13] E.K. Storms, *The refractory carbides*, UK Academic press, London, 1967.
- [14] N.A. Dubrovinskaia, et al., High-pressure study of titanium carbide, *J. Alloy Comp.* 289 (1999) 24–27, [https://doi.org/10.1016/S0925-8388\(99\)00159-0](https://doi.org/10.1016/S0925-8388(99)00159-0).
- [15] H.J. Seifert, et al., *J. Phase Equilib.* 17 (1996) 24–35, <https://doi.org/10.1007/BF02648366>.
- [16] Y. Sun, et al., Cr<sub>3</sub>C<sub>2</sub> assisted ultrafast high-temperature sintering of TiC, *J. Euro. Ceram. Soc.* 43 (2023) 5458–5465, <https://doi.org/10.1016/j.jeurceramsoc.2023.05.031>.
- [17] C. Benoit, TiC nucleation/growth processes during SHS reactions, *Pow. Tech.* 157 (2005) 92–99, <https://doi.org/10.1016/j.powtec.2005.05.035>.